Kinetic behavior of subsonic solitary wave in graphene nanoribbon



J. Stat. Mech. (2015) P06007

(http://iopscience.iop.org/1742-5468/2015/6/P06007)

Journal of Statistical Mechanics: Theory and Experiment
An IOP and SISSA journal

# Kinetic behavior of subsonic solitary wave in graphene nanoribbon

**Jige Chen[1], Wenpeng Qi[1], Meng Zhang[1] and Hong Zhao[2]**

[1] Division of Interfacial Water and Key Laboratory of Interfacial Physics and Technology, Shanghai Institute of Applied Physics, Chinese Academy of Sciences, Shanghai 201800, People's Republic of China
[2] Department of Physics, Institute of Theoretical Physics and Astrophysics, Xiamen University, Xiamen 361005, People's Republic of China
E-mail: chenjige@sinap.ac.cn

Received 30 January 2015
Accepted for publication 12 May 2015
Published 3 June 2015

Online at stacks.iop.org/JSTAT/2015/P06007
doi:10.1088/1742-5468/2015/06/P06007

**Abstract.** In this paper we investigate the kinetic behavior of subsonic solitary waves in graphene nanoribbons by means of molecular dynamics simulations. Unlike generating the supersonic solitary waves by a strong excitation, we generate three types of subsonic solitary waves by absorbing the thermal fluctuations in the armchair and zigzag graphene nanoribbons. They are localized in longitudinal, transverse, or coupled in both velocity directions with propagation speeds lower than the sound speeds. Their typical width is about 20–80 nm, which is much longer than the width of the supersonic solitary wave. More interestingly, they correspond to energy cavities rather than energy summits in the energy distribution due to the deformation in the density distribution. The observation of subsonic solitary waves with energy cavities implies the numerical evidence of dark solitary waves in graphene. Furthermore, the collisions between two solitary waves are investigated. The nonlinear phase shift only occurs during the collision of two solitary waves localized in the same velocity direction. We hope our results shed light on understanding the particular nonlinear properties of graphene.

**Keywords:** transport processes / heat transfer (theory), molecular dynamics


1742-5468/15/P06007+09$33.00

## Contents



## 1. Introduction

Solitary waves are localized particle-like wavepackets, which preserve their identities such as shape and amplitude during propagation and after collision between them due to the compensation of nonlinearity for dispersion. Nowadays, solitary waves are under intense investigation in many nonlinear systems including Bose–Einstein condensates, nonlinear optics, plasmas and anharmonic lattices, etc [1–5].

Graphene, as a unique nonlinear material composed by a single layer of carbon atoms, is known to have many remarkable physical properties due to its strong nonlinearity [6, 7]. For example, thermal rectification is observed in asymmetric mass-loaded/shape distributed graphene and carbon nanotubes [5, 8–12], and thermal conductivity of graphene is found to be length-dependent in suspended graphene [13–15], and several nonlinear optical effects are predicted to be associated with the effective nonlinearity of photonic structures with graphene [16, 17], etc. The ability to support solitary waves in graphene attracts much interest and two kinds of solitary waves are invoked, i.e. the supersonic and subsonic solitary waves. Due to the supersonic feature, that the propagation speed is higher than the sound speed, the supersonic solitary waves in graphene and carbon nanotubes have been intensely investigated in literature over the last decades [18–22]. For example, in molecular dynamics simulations, the supersonic KdV (Korteweg-de Vries) solitary waves can be generated by a strong excitation exerted upon the graphene and carbon nanotubes. Since they are supersonic, it would be easy to distinguish them from the following excited thermal fluctuations. A theoretical model by simplifying the carbon nanotubes and graphene as a monoatomic chain was proposed, which obtains the corresponding KdV equation. On the other hand, theoretical studies indicate the existence of another kind of solitary waves, i.e. the subsonic solitary waves derived from the nonlinear Schrödinger (NLS) equation [23–25]. However, the subsonic feature means their propagation speed is lower than thermal fluctuations, thus it would be much difficult to distinguish them from thermal fluctuations. Up to now, the numerical



J. Stat. Mech. (2015) P06007

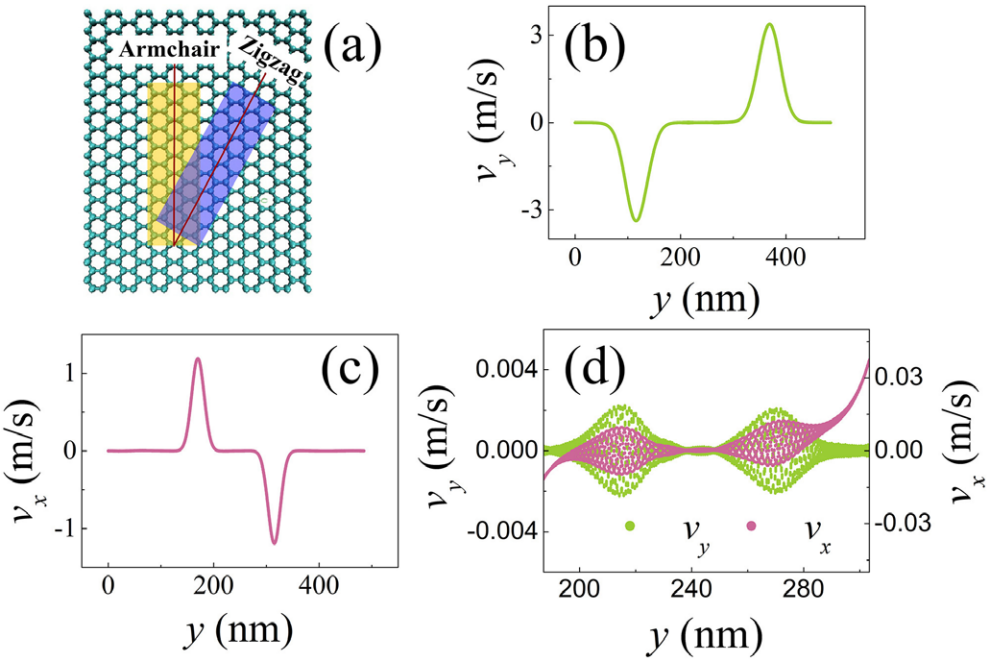


**Figure 1.** (a) Schematic of the armchair and zigzag graphene nanoribbons. The longitudinal direction is along the $y$-axis, and the transverse direction is along the $x$-axis. ((b), (c)) A pair of longitudinal solitary waves (b) and a pair of transverse solitary waves (c) transport along the $y$-axis in the armchair graphene nanoribbon. (d) A pair of longitudinal-transverse coupled solitary waves along the $y$-axis.

observation of the subsonic solitary waves and their kinetic behavior are still unexplored in molecular dynamics simulations.

In this paper, by molecular dynamics simulations, we generate three types of subsonic solitary waves by absorbing the thermal fluctuations in the armchair and zigzag graphene nanoribbons. Comparing with the supersonic solitary waves, they exhibit quite long widths, which is about 20–80 nm. Interestingly, they correspond to energy cavities rather than energy summits in the energy distribution. It indicates they might be the dark solitary waves. Their transportation and collision are also discussed. It is found that the nonlinear phase shift only occurs during the collision of two solitary waves localized in the same velocity direction.

## 2. Methods

We carry out the molecular dynamics simulations in two rectangle graphene nanoribbons with different chirality. As shown in figure 1(a), the armchair and zigzag graphene nanoribbons are denoted by the longitudinal edges along the $y$-axis. The transverse direction is defined along the $x$-axis. The graphene nanoribbons are 485 nm long along the $y$-axis and 4.7 nm wide along the $x$-axis. Periodic boundary condition is used in all directions, which allows the solitary waves to propagate arbitrary long distance without boundary scattering.

We use the adaptive intermolecular reactive empirical bond order (AIREBO) potential [26] as implemented in LAMMPS [27] to simulate the anharmonic coupling between the carbon atoms. We take 1 fs as the minimum time step. The AIREBO potential consists of three terms:

$$E = \frac{1}{2}\sum_{i}\sum_{j\neq i}[E_{ij}^{\mathrm{REBO}} + E_{ij}^{LJ} + \sum_{k\neq i,\, l\neq i,j,k} E_{ijkl}^{\mathrm{TORSION}}] \tag{1}$$

The REBO term has the same functional form as the hydrocarbon REBO potential developed by Brenner [28] with the same coefficients, and it describes the short-ranged C–C covalent bonded interactions. The LJ term adds longer-ranged interactions using a form similar to the standard Lennard Jones potential. The TORSION term is an explicit 4-body potential that describes various dihedral angle preferences in hydrocarbon configurations.

We first thermalize the graphene nanoribbons at a given temperature (e.g. 300 K) for 100 picoseconds with Nose–Hoover thermal bath, and then relax them for 20 picoseconds to be equilibrated. Nonlinear interactions are actuated along side with the thermal fluctuations. In order to observe the subsonic solitary waves, whose propagation speed is lower than the sound speed, the thermal fluctuations have to be suppressed to a low magnitude. Therefore, after the relaxation process, instead of exerting a strong excitation, we absorb the kinetic energy of the thermal fluctuations on the graphene nanoribbons for 1 ns. Such absorbing method is usually used to investigate breathers, whose propagation speed might also be lower than the sound speed, in low-dimensional atomic chains [29,30]. Various solitary waves emerge from the graphene nanoribbons under different initial temperature and absorbing pace by independent simulations. Due to the momentum conservation, here the subsonic solitary waves are usually obtained in pairs.

The solitary waves are characterized by their longitudinal velocity distribution and transverse velocity distribution respectively. The velocity distributions of the carbon atoms are measured as: (1) the longitudinal velocity $v_y$, and (2) the transverse velocity $v_x$. We also investigate the energy distribution, which is stimulated by the solitary waves as:

$$\Delta E = (E_{\mathrm{k}} + E_{\mathrm{p}}) - E_0 \tag{2}$$

where $E_{\mathrm{k}}$ and $E_{\mathrm{p}}$ is the kinetic energy and potential energy of the carbon atoms, and $E_0$ is the average energy of the carbon atoms away from the perturbation of the solitary waves. We also investigate the density distributions, which is stimulated by the solitary waves as:

$$\Delta M = 1.99 \times \frac{4\sqrt{3}}{9} \times \frac{1}{\langle r^2\rangle} - M_0 \tag{3}$$

where $\langle r\rangle$ is the average bond length of each carbon atom between its three neighboring atoms, and $M_0$ is the average density away from the perturbation of the solitary waves.

## 3. Results and discussion

In figure 1(b) we show that three types of subsonic solitary wave are generated in the graphene nanoribbons. For their subsonic feature, it shall be discussed later by investigating their transportation and collision in figures 3 and 4. By their velocity distributions, we can characterize them as (1) the longitudinal solitary wave, and (2)



J. Stat. Mech. (2015) P06007

the transverse solitary wave, and (3) the longitudinal-transverse coupled solitary wave. The term longitudinal and transvers are used to denote localization along the direction of atomic velocity distribution $v_x$ and $v_y$ respectively.

As illustrated in figure 1(b), the subsonic solitary waves have a long width, which differentiate them from the supersonic solitary waves with a short width in literature. The typical width of the longitudinal and transverse solitary waves is about 40–80 nm. And for the longitudinal-transverse coupled solitary wave, its width is about 20–40 nm, which is about one half of the width of the longitudinal or transverse solitary wave. Therefore, their width is about 4–8 times larger than the supersonic solitary waves, whose typical width is only 1–10 nm [18, 19]. Besides, the long width of the subsonic solitary wave is comparable with the mean free path of phonons in graphene, which is about 700 nm at room temperature [31, 32]. It indicates a large scale is needed in molecular dynamics simulations if one tends to consider the contribution of the subsonic solitary waves in graphene nanoribbons.

Meanwhile, for the longitudinal and transverse solitary waves, the amplitude in the velocity distribution of the carbon atoms is about 1–5 $\mathrm{m\,s^{-1}}$. For the longitudinal-transverse coupled localization, the amplitude in the velocity distribution of the carbon atoms is around 0.005–0.05 $\mathrm{m\,s^{-1}}$, which implies the coupling of longitudinal and transverse modes would dramatically weaken the amplitudes of nonlinear interaction. Furthermore, we have only observed random fluctuation in out-of-plane velocity distribution. Such dynamical difference reveals the separate impact of the flexural modes (out-of-plane vibrations) upon the nonlinear properties in the graphene nanoribbons [31–33].

Energy localization is usually investigated to characterize the kinetic properties of the solitary waves. For example, the supersonic solitary waves exhibit a high-energy localization due to their excited kinetic energy. Thus they are usually referred to be bright solitary waves [2, 3, 18, 19, 34]. In figure 2(a), we show the energy distribution of a pair of longitudinal solitary waves, and a pair of longitudinal-transverse coupled solitary waves. Interestingly, they exhibit energy cavities rather than energy summits, which is referred to be dark solitary waves [1–3, 34]. Since the energy distribution is the sum of kinetic energy and potential energy, density deformation should be observed in the graphene nanoribbons in order to obtain a negative potential energy. Therefore, in figures 2(a) and (b), we investigate the density distribution of the longitudinal solitary waves and longitudinal-transverse coupled solitary waves to illustrate such deformation. An aggregation in the density distribution is observed, which leads to the cavity in the energy distribution. Our observation of energy cavities provides a numerical evidence of possible dark NLS solitary waves in graphene, which has been only theoretically proposed in literature. Furthermore, the coupling of longitudinal and transverse modes also weakens the amplitude of solitary waves in the energy distribution. The magnitude of longitudinal-transverse coupled solitary wave is quite smaller than the longitudinal or transverse solitary waves.

In figure 3, we illustrate the transportation of the longitudinal solitary waves with different amplitudes. Similar transportation behavior is also observed in the transverse solitary waves. Their identities, such as shape and amplitude, remain invariant during the transportation process. Their propagating speeds are weakly dependent upon their amplitudes for a short range of time. The propagating speed of a longitudinal solitary wave



J. Stat. Mech. (2015) P06007

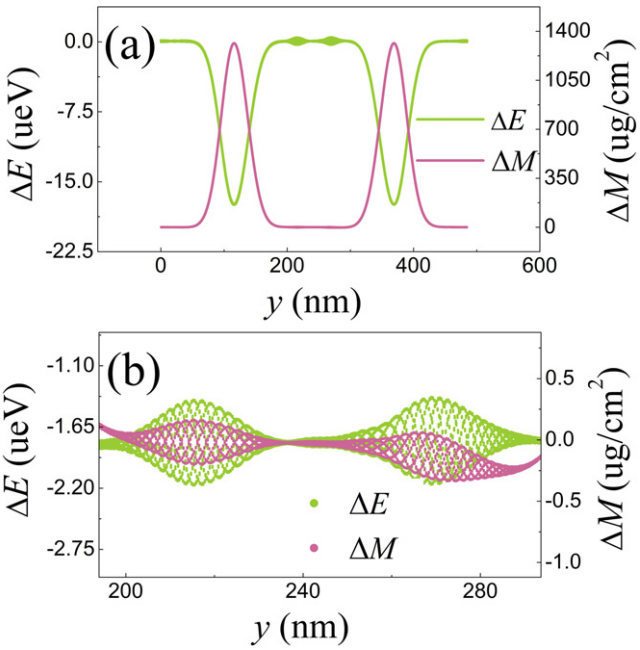


**Figure 2.** (a) The energy and density distribution of the longitudinal solitary waves in the armchair graphene nanoribbon. A pair of longitudinal-transverse coupled solitary waves is illustrated in the middle. (b) The energy and density distribution of the longitudinal-transverse coupled solitary waves.

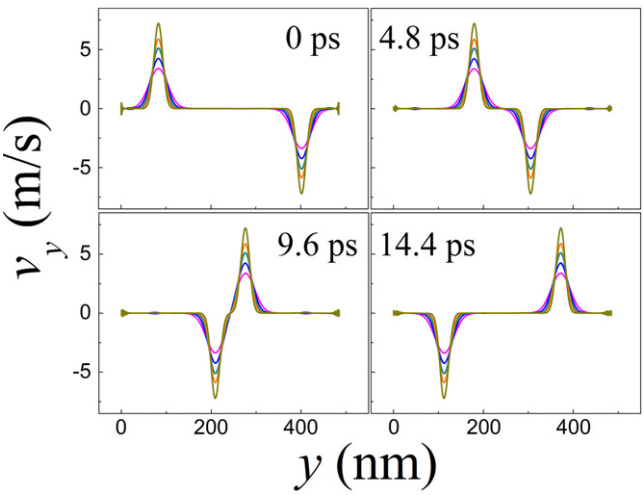


**Figure 3.** The propagation of the longitudinal solitary waves with various amplitudes in the armchair graphene nanoribbons. The time interval is 4.8 ps. Their identities, such as shape and amplitude, remain invariant during such the transportation process.

is 20.0 km s$^{-1}$ and the propagating speed of a transverse solitary wave is 11.4 km s$^{-1}$. Both velocities are smaller than the relative sound speeds, which are 21.3 km s$^{-1}$ (longitudinal sound speed) and 13.6 km s$^{-1}$ (transverse sound speed) in graphene nanoribbons [33]. It was theoretically proposed that the high solitary wave speed corresponds to a short width

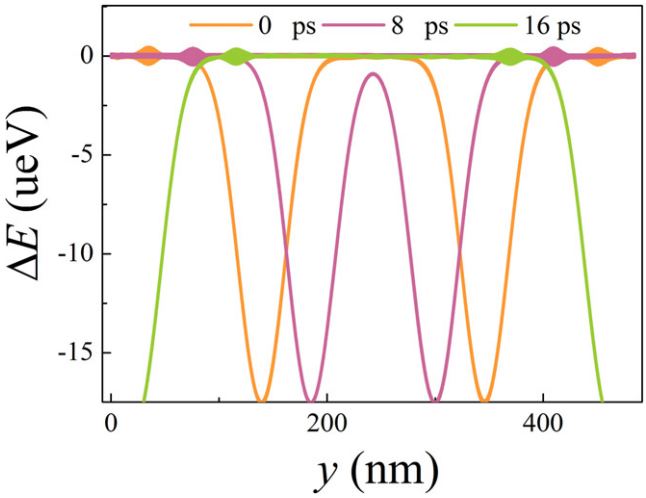


**Figure 4.** The propagation of a pair of longitudinal-transverse coupled solitary waves. The time interval is 8 ps. Their shapes and amplitudes remain invariant in the transportation process.

and small amplitude [18, 19]. Therefore, the observed low propagation speed explains the origin of the long width and small amplitude as illustrated in figure 1.

Similarly, in figure 4, we illustrate the transportation of a pair of longitudinal-transverse coupled solitary waves. Their shapes and amplitudes remain invariant during the transportation process. The propagating speed value is $5\,\mathrm{km\,s^{-1}}$, which is smaller than either the longitudinal or the transverse sound speed ($21.3\,\mathrm{km\,s^{-1}}$ and $13.6\,\mathrm{km\,s^{-1}}$). It implies that the coupling of longitudinal and transverse modes would significantly decrease the propagating speed of the solitary waves in the graphene nanoribbons.

During the collision between two solitary waves, they would strongly interact with each other due to nonlinearity. After the collision process, the solitary waves emerge again with energy scattering and a nonlinear phase shift [34–36]. The energy scattering means that an amount of energy of the solitary wave would be scattered as thermal fluctuations into the low-amplitude oscillations. It is due to fact that the theoretical graphene model is a non-integrable discrete model based upon the interaction between separate carbon atoms. Only an integrable continuum model with exact soliton solutions is able to exclude the energy scattering, where the solitary wave could be referred as a soliton. Phase shift means that a spatial-temporal jump would deviate the spatial-temporal trajectory of the solitary waves. If one extends the original trajectory of a solitary wave before the collision, the original trajectory is a line parallel to the after-collision trajectory with a definite distance away. Phase shift indicates the interactions of nonlinearity, which distinguishes it from superposed linear interaction. In figure 4(a), we take the collision process between two longitudinal solitary waves as an example to illustrate the nonlinear interactions between them. During the collision, their amplitudes $|v_y|$ deform due to their interactions. After collision, their amplitudes decreases due to the energy lost. Therefore, we measure the energy scattering according to the kinetic energy change as $\sum v_y^2(0) - \sum v_y^2(t)/\sum v_y^2(0)$, where $v_y(0)$ and $v_y(t)$ indicates the atomic velocity of the carbon atoms in a solitary wave before and after the collision respectively. Here about 2% energy scattering is observed in one collision process. Meanwhile, in figure 4(b), we show that the spatial-temporal

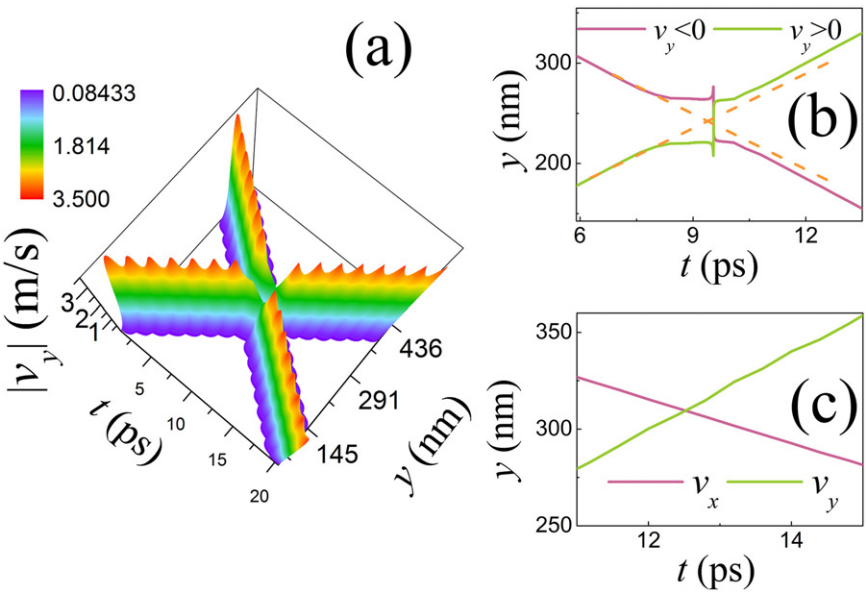


**Figure 5.** (a) The spatial-temporal trajectories of two longitudinal solitary waves. They interact strongly with each other during the collision process. (b) The spatial-temporal jump is observed in the spatial-temporal trajectories. It corresponds to the phase shift between two longitudinal solitary waves. (c) The spatial-temporal trajectories between a longitudinal and a transverse solitary wave. No phase shift occurs during the collision process.

jump occurs during the collision process of the two solitary waves. To investigate the phase shift, we further extend the two original trajectories of the solitary waves before the collisions (the orange dash lines). The two extended lines are parallel to the two after-collision trajectories (red and green lines). Comparing with the after-collision trajectories, the extended lines are adjacent to each other with less distance away. Such behavior indicates the two solitary waves are accelerated in the collision process. On the other hand, as illustrated in figure 5(c), no nonlinear interaction occurs in the collision process between a longitudinal and a transverse solitary waves. They just pass through each other without any spatial-temporal jumps. It implies that the phase shift only occurs between two solitary waves, which are localized in the same velocity direction.

## 4. Conclusion

In summary, we generate three types of subsonic solitary waves in graphene nanoribbons by molecular dynamics simulations. They are longitudinal, transverse, and longitudinal-transvers coupled solitary waves. They exhibit low propagation speeds and long widths. Unlike the supersonic solitary waves, their energy localizations exhibit cavities rather than summits due to the deformation in the density distribution. Such characteristic indicates they correspond to dark solitary waves. Their collision process is investigated by considering the energy lost and the phase-shift in the spatial-temporal trajectories. Our results might be helpful to understand the particular nonlinear properties of graphene.

## Acknowledgments

This work was supported by National Natural Science Foundation of China (#11405245), and Shanghai Natural Research Funding (#14ZR1448100), and the Key Research Program of Chinese Academy of Sciences (#KJZD-EW-M03). The authors also thank the Knowledge Innovation Program of the Chinese Academy of Sciences, Shanghai Supercomputer Center of China, the Deepcomp7000 and ScGrid of super-computing Center, Computer Network Information Center of Chinese Academy of Sciences.

## References

[1] Becker C, Stellmer S, Soltan-Panahi P, Dorscher S, Baumert M, Richter E-M, Krongager J, Bongs K and Sengstock K 2008 *Nat. Phys.* **4** 496
[2] Lederer F, Stegeman G I, Christodoulides D N, Assanto G, Segev M and Silberberg Y 2008 *Phys. Rep.* **463** 1
[3] Heidemann R, Zhdanov S, Sütterlin R, Thomas H M and Morfill G E 2009 *Phys. Rev. Lett.* **102** 135002
[4] Zhao H, Wen Z, Zhang Y and Zheng D 2005 *Phys. Rev. Lett.* **94** 025507
[5] Chang C W, Okawa D, Majumdar A and Zettl A 2006 *Science* **314** 1121
[6] Geim A K 2009 *Science* **324** 1530
[7] Neto A H C 2010 *Mater. Today* **13** 12
[8] Alaghemandi M, Algaer E, Böhm M C and Müller-Plathe F 2009 *Nanotechnology* **20** 115704
[9] Alaghemandi M, Leroy F, Algaer E, Böhm M C and Müller-Plathe F 2010 *Nanotechnology* **21** 075704
[10] Alaghemandi M, Leroy F, Müller-Plathe F and Böhm M C 2010 *Phys. Rev.* B **81** 125410
[11] Cheh J and Zhao H 2011 *J. Stat. Mech.* P10031
[12] Cheh J and Zhao H 2012 *J. Stat. Mech.* P06011
[13] Xu X *et al* 2014 *Nat. Commun.* **5** 3689
[14] Savin A V, Hu B and Kivshar Y S 2009 *Phys. Rev.* B **80** 195423
[15] Guo Z, Zhang D and Gong X-G 2009 *Appl. Phys. Lett.* **95** 163103
[16] Gullans M, Chang D E, Koppens F H L, de Abajo F J G and Lukin M D 2013 *Phys. Rev. Lett.* **111** 247401
[17] Smirnova D A, Gorbach A V, Iorsh I V, Shadrivov I V and Kivshar Y S 2013 *Phys. Rev.* B **88** 045443
[18] Astakhova T Y, Gurin O D, Menon M and Vinogradov G A 2001 *Phys. Rev.* B **64** 035418
[19] Astakhova T Y, Menon M and Vinogradov G A 2004 *Phys. Rev.* B **70** 125409
[20] Savin A V and Savina O I 2004 *Phys. Solid State* **46** 383
[21] Savin A V and Kivshar Y S 2010 *Europhys. Lett.* **89** 46001
[22] Braghin F L 2013 *Eur. Phys. J.* B **86** 75
[23] Bludov Y V, Smirnova D A, Kivshar Y S, Peres N M R and Vasilevskiy M I 2015 *Phys. Rev.* B **91** 045424
[24] Suntsov S, Makris K G, Christodoulides D N, Stege-man G I, Hach A, Morandotti R, Yang H, Salamo G and Sorel M 2006 *Phys. Rev. Lett.* **96** 063901
[25] Rosberg C R, Neshev D N, Krolikowski W, Mitchell A, Vicencio R A, Molina M I and Kivshar Y S 2006 *Phys. Rev. Lett.* **97** 083901
[26] Stuart S, Tutein A and Harrison J A 2000 *J. Chem. Phys.* **112** 6472
[27] Plimpton S 1995 *J. Compt. Phys.* **117** 1
[28] Brenner D W, Shenderova O A, Harrison J A, Stuart S J, Ni B and Sinnott S B 2002 *J. Phys.: Condens. Matter* **14** 783
[29] Xiong D, Zhang Y and Zhao H 2013 *Phys. Rev.* E **88** 052128
[30] Xiong D, Zhang Y and Zhao H 2014 *Phys. Rev.* E **90** 022117
[31] Ghosh S, Calizo I, Teweldebrhan D, Pokatilov E P, Nika D, Balandin A A, Bao W, Miao F and Lau C N 2008 *Appl. Phys. Lett.* **92** 151911
[32] Cai W, Moore A L, Zhu Y, Li X, Chen S, Shi L and Ruoff R S 2010 *Nano Lett.* **10** 1645
[33] Nika D L, Pokatilov E P, Askerov A S and Balandin A A 2009 *Phys. Rev.* B **79** 155413
[34] Drazin P G and Johnson R S 1989 *Solitons: An Introduction* 2nd edn (Cambridge: Cambridge University Press)
[35] Ikezi H, Taylor R and Baker D R 1970 *Phys. Rev. Lett.* **25** 11
[36] Jin T, Zhao H and Hu B 2010 *Phys. Rev.* E **81** 037601



J. Stat. Mech. (2015) P06007